chemosensors

MDPI

Review

Estimation of Enantiomeric Excess Based on Rapid Host–Guest Exchange

Jan Labuta [1,*], Shinsuke Ishihara [1,*], Daniel T. Payne [2], Kazuyoshi Takimoto [3], Hisako Sato [3], Lenka Hanyková [4], Katsuhiko Ariga [1] and Jonathan P. Hill [1,*]

1 International Center for Materials Nanoarchitectonics, National Institute for Materials Science, Namiki 1-1, Tsukuba 305-0044, Japan; ARIGA.Katsuhiko@nims.go.jp
2 International Center for Young Scientists, National Institute for Materials Science, Namiki 1-1, Tsukuba 305-0044, Japan; Payne.Daniel@nims.go.jp
3 Graduate School of Science and Engineering, Ehime University, Matsuyama 790-8577, Ehime, Japan; g865002h@mails.cc.ehime-u.ac.jp (K.T.); sato.hisako.my@ehime-u.ac.jp (H.S.)
4 Department of Macromolecular Physics, Faculty of Mathematics and Physics, Charles University, V Holešovičkách 2, 180 00 Prague, Czech Republic; Lenka.Hanykova@seznam.cz
* Correspondence: Labuta.Jan@nims.go.jp (J.L.); ISHIHARA.Shinsuke@nims.go.jp (S.I.); jonathan.hill@nims.go.jp (J.P.H.)

Abstract: Chiral molecules possess enantiomers that have non-superimposable chemical structures but exhibit identical nuclear magnetic resonance (NMR) spectra. This feature prevents the use of NMR spectroscopic methods for the determination of enantiomeric excesses (*ee*) of chiral molecules, using simple mixtures of their enantiomers. Recently, however, it was reported that the addition of a symmetrical prochiral molecule (a reporter or host) into a solution of chiral analyte can lead to estimation of *ee* through interactions involving rapid exchange of the chiral analyte (guest) in the formed host–guest complex. This is due to the *ee*-dependent splitting of NMR resonances of the prochiral host molecule based on averaging the chemical shift non-equivalency caused by the presence of a chiral guest. The mechanism is not dependent on diastereomer formation, and 1:1 host–guest complexes can also show *ee*-dependent NMR peak splitting. Prochiral molecules capable of *ee* sensing using the NMR technique are now referred to as so-called prochiral solvating agents (*pro*-CSAs). *pro*-CSAs represent a family of reagents distinct from the commonly used NMR chiral derivatizing reagents (where chiral auxiliaries are used to derivatize enantiomers to diastereomers) or chiral solvating agents (where chiral auxiliaries interact in an asymmetric manner with analyte enantiomers). *pro*-CSA methods are unique since neither *pro*-CSA nor NMR contains chiral factors, making the technique neutral with respect to chirality. Here, we review our recent work on this matter involving several different nominally achiral receptor molecules whose unique guest binding properties and solution characteristics (especially with regard to NMR spectroscopy) allow for the estimation of *ee* in the corresponding chiral guests.

Keywords: chirality; enantiomeric excess; NMR spectroscopy; prochiral solvating agent; fast host–guest exchange

check for updates

Citation: Labuta, J.; Ishihara, S.; Payne, D.T.; Takimoto, K.; Sato, H.; Hanyková, L.; Ariga, K.; Hill, J.P. Estimation of Enantiomeric Excess Based on Rapid Host–Guest Exchange. *Chemosensors* **2021**, *9*, 259. https://doi.org/10.3390/chemosensors9090259

Academic Editor: Marco Frasconi

Received: 12 August 2021
Accepted: 7 September 2021
Published: 9 September 2021

Publisher's Note: MDPI stays neutral with regard to jurisdictional claims in published maps and institutional affiliations.

Copyright: © 2021 by the authors. Licensee MDPI, Basel, Switzerland. This article is an open access article distributed under the terms and conditions of the Creative Commons Attribution (CC BY) license (https://creativecommons.org/licenses/by/4.0/).

1. Introduction

Chirality not only plays a critical role in biochemical reactions, but also is an important consideration in the development of novel medicines [1], asymmetric syntheses [2], including catalysis [3,4], and molecular self-assembling systems [5–10]. For these reasons, the detection and analysis of molecular chiral activity, including the relative purities of chiral substances and their interactions, is a burgeoning research area of increasing importance due to the overarching role of asymmetry and stereochemistry [11,12]. Several analytical techniques for the determination of chiral characteristics are known and are widely applied, including gas chromatography (GC) [13], high performance liquid chromatography (HPLC) [14–17] and nuclear magnetic resonance (NMR) spectroscopy [18–20].

Notable methods of chiral analysis involving spectroscopic and similar methods include several techniques, involving circular dichroism (CD) [21–23], electronic spectroscopy (e.g., ultraviolet-visible (UV-vis) [24–26], fluorescence (Fl) [27–30]) and cyclic voltammetry (CV) [31], usually with a chiral host molecule for detection. Achiral hosts, where diastereomer complexes are observed [32] or where helicity is induced in chromophore dimer molecules by complexation with chiral guests, have also been studied [33–36]. As a result of the presence of isomers, chiral compounds exhibit enantiomeric excess (*ee*), a measure of their purity with respect to chiral isomer content. This important parameter can determine the effectiveness of a chiral therapeutic agent [37], or it can be used as an index to assess the success of reactions involving chiral products, especially those involving asymmetric catalysts [38]. While the aforementioned GC [13] and HPLC [14–17] methods are very useful for the evaluation of *ee*, NMR spectroscopy can also be used for this purpose by using three common protocols: (a) analyte derivatization with a chiral modifier [39–41], (b) lanthanide-containing shift reagents [40], and (c) the addition of a chiral solvating agent (CSA) [40,41]. The latter involves the formation of diastereomeric complexes with the different enantiomers of analytes. In the case of NMR spectroscopy, until relatively recently, it was not possible to use it to analyze *ee* without using an intrinsically chiral analytical probe substance because NMR is essentially insensitive to the enantiomer identity.

Our work on this subject, which is the topic of this review, was initially based on non-chiral CSA, where information about *ee* is extracted based on the enantiotopicity of host proton NMR resonances in rapidly exchanging guests in guest–host complexes [42–44]. The mechanism of the *ee* detection was also confirmed by applying computational methods, including molecular dynamics simulations [43,44]. Subsequently, we have also considered other corresponding small molecule systems [45] as well as receptors from the now well-established porphyrin dimer family [46] and coordination complexes [47]. The latter are highly promising as analytical reagents because of the large available range of ligand–metal cation combinations, which can be adapted for analyses under many different conditions. Here, we present an overview of our recent work on *ee* estimation. It is given in largely chronological order to illustrate how our philosophy has progressed during consideration of this subject. Initial observations in the oxoporphyrinogen (**OxP**) system were developed, eventually yielding an achiral host, while similar activity was found in *meso*-tetraphenylporphyrin (**TPP**) dications. Sensing activity was also found in selected small molecule systems and coordination complexes of zinc (II). Finally, we considered the sensing activities of a chiral porphyrin dimer using several different spectroscopic techniques to emphasize the utility of those molecules. Chemical structures of the *ee*-sensing probes described here are shown in Figure 1. The *ee* sensing activity of these probes provides insights into interactions between chiral species and both the achiral and chiral host systems shown. Furthermore, the host–guest systems are complementary to existing techniques for chiral analysis, such as GC/HPLC and the other well-established NMR methods.

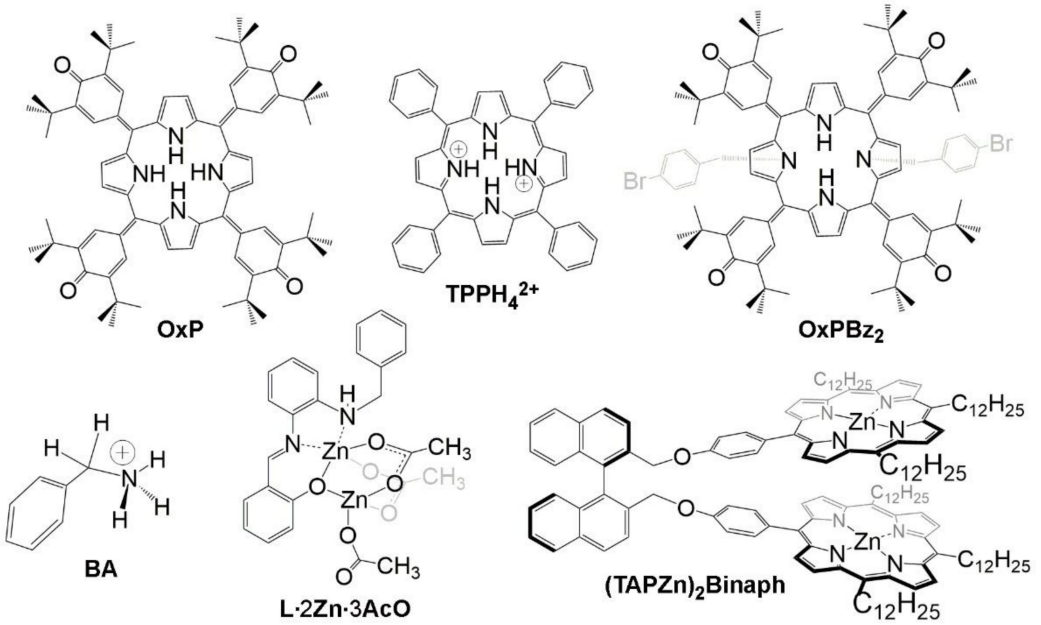

Figure 1. Chemical structures of the probe molecules: 5,10,15,20-*tetrakis*(3,5-di-*t*-butyl-4-oxocyclohexa-2,5-dienylidene)porphyrinogen (**OxP**); 5,10,15,20-tetraphenylporphyrin dication (**TPPH$_4^{2+}$**); $N_{21}N_{23}$-bis(4-bromobenzyl)-5,10,15,20-*tetrakis*(3,5-di-*t*-butyl-4-oxocyclohexa-2,5-dienylidene)porphyrinogen (**OxPBz$_2$**); benzylammonium (**BA**); salen-Zn_2 acetate bridged dimer (**L·2Zn·3AcO**); 1,1′-binaphthyl trialkylporphyrinatozinx (II) cofacial dimer (**(TAPZn)$_2$Binaph**).

2. Oxoporphyrinogens and Porphyrin Dications

Oxoporphyrinogens (**OxP**, 5,10,15,20-*tetrakis*(3,5-di-*t*-butyl-4-oxocyclohexa-2,5-dien ylidene)porphyrinogen [48,49]) derived from the 2-electron oxidation of 5,10,15,20-*tetrakis*(3,5-di-*t*-butyl-4-hydroxyphenyl)porphyrin [50] are a class of tetrapyrroles related to, but apart from, the calix[4]pyrroles [51]. They have been studied for their interactions with anions [52], anion–cation pairs [53], water [54], and other analytes [55–57] as components of multichromophore systems as an electron acceptor [58–62], and also as H-bonding catalysts [63]. Their saddle-like structures allow for hydrogen bonding interactions with a wide variety of potential analytes, which can also lead to changes in the electronic absorption spectra of the chromophore incorporated in the macrocyclic framework. We first observed a response to chiral analytes in the simplest of **OxP**-type probe molecules '**OxP**', although the macrocycle dynamics and tautomeric processes of that compound obscured the intrinsic chiral characteristics of this molecule. These matters could be eliminated synthetically, yielding a truly achiral molecule subsequently used for enantiomeric excess determinations.

The porphyrins [64], a family of tetrapyrrole macrocycles and their metal complexes, have significant photochemical and catalytic properties as illustrated, respectively, by the chlorophylls [65] and heme [66]. Additionally, certain synthetic porphyrins are adapted as chiral sensing molecules because their usually strong electronic absorption in UV and visible regions allows observations of the local environments, using CD spectrophotometry. This field has been established due to work from Nakanishi [67], Berova [35,68], Inoue [69], and Borovkov [32], amongst others; these studies have made it clear that a site for supramolecular interaction is critical for the activity of any prospective chiral sensing molecules. For us, the molecule **OxP** [48,49] presented such an opportunity, due to the presence of hydrogen bonding guest binding site(s), and it is also highly colored (and can provide colorimetric/optical or electrochemical responses [62,70]). While there exists a large body of reports about chiral analysis using porphyrins in conjunction with CD spectroscopy and other methods [71], there are only a few accounts regarding the same purpose involving NMR spectroscopy.

The structure of **OxP** [50] reveals a saddle-shape conformation of the pyrrole groups in the molecule. **OxP** interacts with guests through H-bonding at its pyrrole NHs, and this was initially investigated for **OxP** interacting with chiral mandelic acid, **MA** (Figure 2) [42]. It was observed by NMR spectroscopy that the presence of excess (9 eq.) racemic mandelic acid (**MA**) together in solution with **OxP** causes resonances, due to *t*-butyl protons, quinonoid alkene protons, and pyrrolic β-proton to shift downfield, while those due to pyrrolic NH are no longer visible (Figure 2b (i,ii)). This is due to the formation of an acid–base complex, **OxP**·2**MA**. On the other hand, if pure (*R*)-enantiomer **MA** is present, both the pyrrolic β proton and quinonoid resonances of the **OxP** host are not only shifted downfield, but also split to two peaks (Figure 2b (iii)). The degree of splitting does not vary (even in the presence of excess **MA**). Therefore, these two peaks originate from the acid–base complex of **OxP** with **MA**. **OxP** behaves similarly in the presence of the (*S*)-enantiomer. Thus, the splitting of peaks is due to the chirality of the guest. Different non-racemic mixtures of **MA** were then applied, leading to the finding that the degree of peak splitting is dependent on the *ee* (Figure 2c). The chemical shift difference ($\Delta\delta$) of the peak splitting was plotted against the respective *ee* values of the analyte (mandelic acid), leading to a linear correlation of these parameters (Figure 2d), indicating that the splitting of NMR peaks of the host is based on a transfer of guest chirality information to the host. As we understood it at the time, this was the initial demonstration of an achiral host as a probe of *ee* operated by considering the $\Delta\delta$ of splitting of its NMR peaks. In the case of chiral hosts, *ee* is estimated by measuring the ratio of guest (i.e., chiral analyte) peak areas, which are distinguishable due to the host–guest diastereomer complex formation [41].

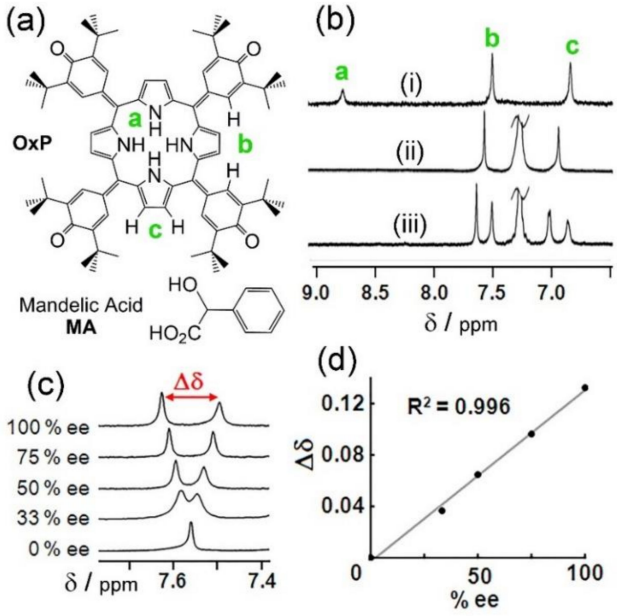

Figure 2. (**a**) Structure of the achiral **OxP** host and chiral mandelic acid **MA** with analytically important protons labelled a–c. (**b**) ^{1}H-NMR spectra of (i) **OxP**, (ii) **OxP** in the presence of 9.3 equivalents of (*rac*)-**MA**, and (iii) **OxP** in the presence of 8.8 equivalents of (*R*)-**MA**. (**c**) **OxP** quinonoid proton resonance (labelled b) in solution with **MA** at different enantiomeric excesses. (**d**) Correlation between *ee* and $\Delta\delta$ for spectra shown in (c). Adapted with permission from ref. [42]. Copyright 2009 American Chemical Society.

Highly colored **OxP** can also be analyzed for physical changes by using other techniques, such as UV-vis or CD spectrophotometry. Purple-to-red color changes are observed in **OxP** solutions when large quantities of either (*R*)- or (*rac*)-**MA** are added (Figure 3a), with resulting solutions having identical UV-vis spectra (Figure 3a) and strong induced CD signals dependent on the chirality of the guest (Figure 3b). The gradual addition of (*R*)-**MA**

leads to the emergence and intensification of a new band around 790 nm with a concurrent weakening and splitting of the **OxP** absorption maximum band around 500 nm.

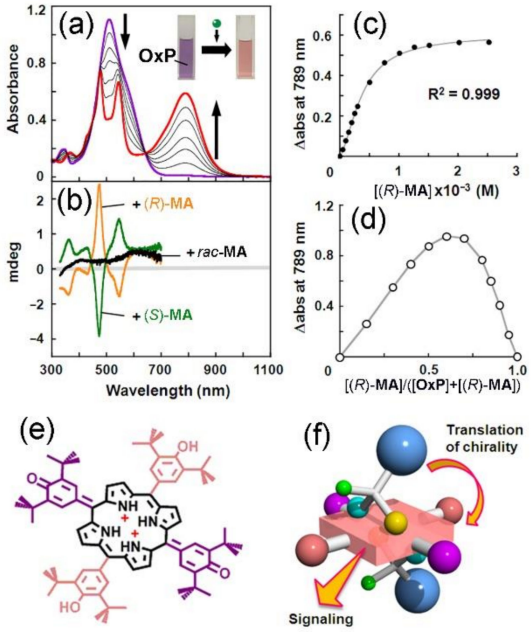

Figure 3. (**a**) Variation in UV-vis spectrum during titration of **OxP** (10^{-5} M, CH_2Cl_2) with (*R*)-**MA.** (**b**) CD spectra of **OxP** (10^{-5} M, CH_2Cl_2) in the presence of respective excesses of (*R*)-, (*S*)- or (*rac*)-**MA**. (**c**) Change of absorbance at 789 nm with (*R*)-**MA** concentration. (**d**) Job's plot of interaction of **OxP** with (*R*)-**MA**. (**e**) Chemical structure of diprotonated tautomer of **OxP**. (**f**) Illustration of the concept of transfer of chiral information from **MA** to the NMR output of the achiral **OxPH$_2$**$^{2+}$ host. Adapted with permission from Ref. [42]. Copyright 2009 American Chemical Society.

A 1:2 stoichiometry (Figure 3c,d) was found for the interaction between **OxP** and **MA** with 1st and 2nd binding constants of $K_1 = 1.3 \times 10^3$ M^{-1} and $K_2 = 5.3 \times 10^3$ M^{-1}, respectively, suggesting positive cooperativity (α) of the binding based on $\alpha = 4K_2/K_1 = 16.3 >> 1$. Note that the formation of **OxP**·2**MA** involves a different mechanism of binding than H-bonded **OxP**-anion complexes [42,44,46], due to the acidity of the guest (**OxP** has a similar spectrum in the presence of methanesulfonic acid, indicating that it is due to protonation). The acid-induced splitting of the 500 nm band in **OxP** complexes indicates a symmetry-breaking process (D_{2d} to D_2), which was assigned to the prototropic tautomerization of **OxP** to its 5,15-porphodimethene form with phenolic and hemiquinonoid substituents (Figure 3e,f). This suggests that the **OxP**·2**MA** complex involves partly electrostatic interactions between diprotonated (cationic tautomer) **OxP** and anions of **MA** as was previously observed for complexes of organic anions with **TPP** dications [62].

For the protonated **OxP**–guest complexes, there are related complicating factors for their analyses [44]. These are macrocyclic inversion (also referred to as 'ring-flip') and prototropic tautomerism, which obstruct rationalization of the *ee*-sensing mechanism involving **OxP** [42]. Protonation of **OxP** changes its structure so that oxocyclohexadienylidene groups at *meso*-positions reversibly interconvert to phenols. **OxP** adopts D_2-symmetry (from D_{2d}) upon protonation with 2 eq. mandelic acid **MA,** leading to the emergence of chirality since saddle-shaped **OxPH$_2$**$^{2+}$ can exist as (+)-**OxPH$_2$**$^{2+}$ and (–)-**OxPH$_2$**$^{2+}$, which are dynamically interconverting enantiomers (Figure 4). The interconversion between these enantiomers occurs by ring-flip and tautomerism mechanisms resembling a known molecular chiral memory [72]. It is interesting to note the use of a chiral guest as a probe of the **OxP** dynamic processes (tautomerism and inversion). Ultimately, in this case, guest chirality allowed us to detect and observe the enantiomers of **OxP** by the formation of diastereomers. However,

it was concluded that these complicating factors make it difficult to establish unequivocally the mechanism of *ee* sensing, and we returned to the synthesis drawing board.

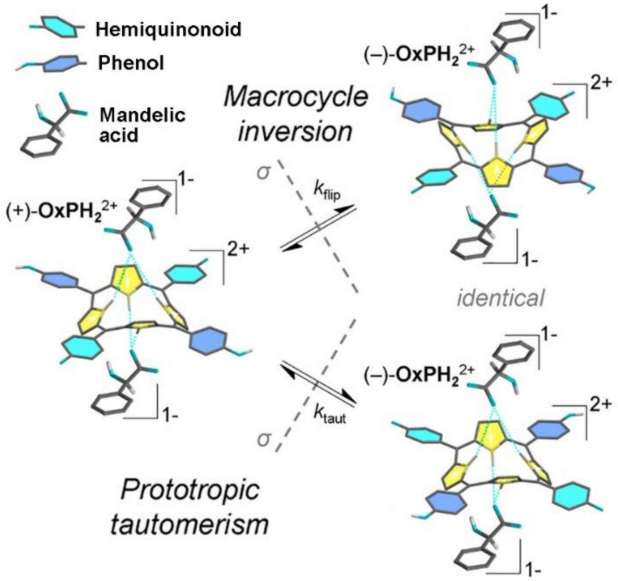

Figure 4. Macrocyclic inversion dynamics (ring-flip) and prototropic tautomers. The (–)-**OxPH$_2$**$^{2+}$ structures at the right are identical (related by a 90° rotation around axes perpendicular to the **OxPH$_2$**$^{2+}$ mean plane). Adapted with permission from Ref. [44]. Copyright 2014 American Chemical Society.

Our work on the initial **OxP** system, although challenging, has led to the development of the prochiral solvating agents (*pro*-CSA) for possible practical application. For **OxP**, hydrogen bonding sites, i.e., pyrrolic NHs, are indispensable, while tautomeric processes are not advantageous, due to possible variations in the host's structure. Tautomeric processes occur because of electronegative atoms at the periphery of **OxP**, so our investigations were continued by checking the possibilities of using simple tetraalkyl- and tetraphenylporphyrin dications, which cannot undergo complicated tautomeric processes (although inversion remains). *Tetrakis* (*t*-butyl) porphyrin (**T*t*BuP**) and tetraphenylporphyrin (**TPP**) were then applied for use as probes of *ee* [73].

At 25 °C, **TPP** does not interact with chiral carboxylic acids in $CDCl_3$. On cooling to −32.5 °C, there are distinct changes in ^{1}H-NMR spectra (Figure 5a) caused by the protonation of **TPP**. This is confirmed by its UV-vis spectrum (Figure 5b). Solutions of **TPP** containing 2-phenoxypropionic acid (**PA**) exhibit a very weak mono-signated CD spectrum (also only on cooling; Figure 5c), suggesting that chiral guest binding causes an insignificant macrocyclic distortion. In ^{1}H-NMR spectra of solutions containing (*R*)-**PA** measured at −32.5 °C, *ortho*-phenyl-H and pyrrole-H resonances of **TPP** are each symmetrically split to two sets of signals (Figure 5d). The degree of splitting ($\Delta\delta$) is dependent on *ee* of the chiral carboxylic acid used. Plots of $\Delta\delta$ against *ee* indicate a linear relationship; $\Delta\delta = \Delta\delta_{max} \times ee$. $\Delta\delta_{max}$ is the characteristic maximum splitting of each chiral acid. Similar to **OxP** [42], ion-pair formation of a 1:2 host–guest complex leads to a linear relationship between $\Delta\delta$ and *ee* at −32.5 °C (Figure 5e). Guest counteranions exchange rapidly at the two available binding sites; the host remains effectively doubly protonated on the NMR timescale.

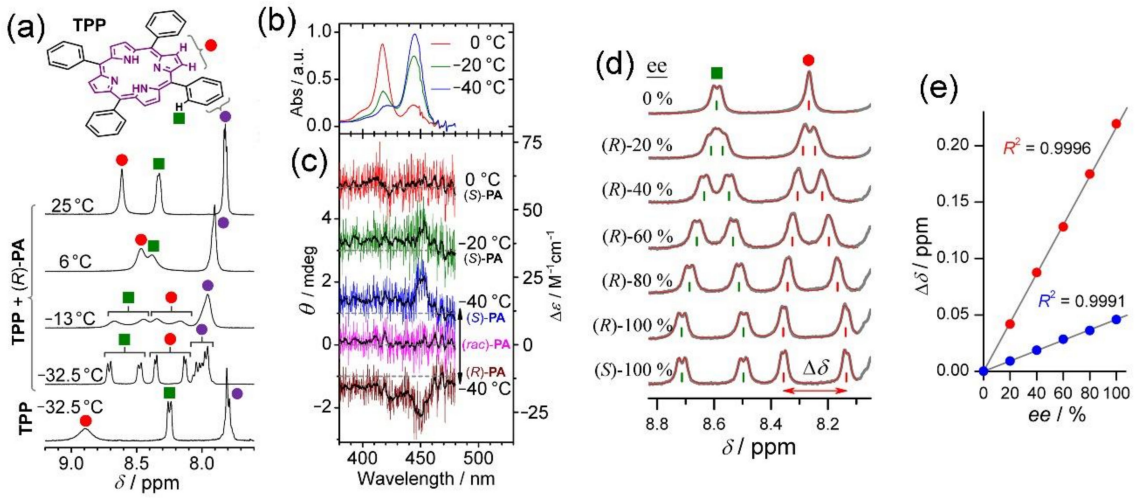

Figure 5. (**a**) ^{1}H-NMR spectra of **TPP** in $CDCl_3$ with 8 equivalents (*R*)-2-phenoxypropionic acid ((*R*)-**PA**) collected while cooling to –32.5 °C (lowest trace shows **TPP** only). A spectrum of $\mathbf{TPPH_4}^{2+}$ (at –32.5 °C: **TPP** + (*R*)-**PA**) differs significantly from free **TPP** at –32.5 °C. (**b**) UV-vis spectra of $\mathbf{TPP}/\mathbf{TPPH_4}^{2+}$ with excess (500 eq.) (*S*)-**PA** on cooling to −40 °C. Absorption at 445 nm due to porphine dication increases on cooling. (**c**) Circular dichroism (CD) spectra of $\mathbf{TPPH_4}^{2+}$ with excess (500 eq.) (*S*)-**PA** during cooling (top 3 traces) and with (500 eq.) (*S*)-**PA**, (*rac*)-**PA**, and (*R*)-**PA** at −40 °C (bottom 3 traces). (**d**) Partial ^{1}H-NMR spectra of the $\mathbf{TPPH_4}^{2+}$ aromatic region (–32.5 °C) in the presence of various *ee* of (*R*)-**PA** used to estimate $\Delta\delta$. (**e**) Dependency of $\Delta\delta$ on *ee* for the porphine β-H resonances of **TPP** in the presence of **PA** (red) or Ibuprofen (blue) showing a linear relationship. Adapted with permission from Ref. [73]. Copyright 2011 John Wiley and Sons.

By making the tetrapyrrole host molecule less complex (by replacing hemiquinonoids of **OxP** with phenyls but keeping the saddle shape of macrocycle–porphyrin dication, it is coincidentally similar to the $\mathbf{TPPH_4}^{2+}$ system [74]), a model mechanism for host–guest interactions in this system could be developed. This model accounts for the linear relationship between $\Delta\delta$ and *ee* [73]. At this point, we noted that **OxP** and porphyrin dications are applicable for analysis only of chiral carboxylic acids. To make the concept more general, a class of compounds whose structures could overcome the disadvantages of the **OxP** and **TPP** systems was sought. The following criteria were applied for the development of the new host and are given in order of increasing importance: (a) room temperature operability (for measurement convenience); (b) should not require protonation or other modification incidental or otherwise to operate as a host (i.e., can interact with a range of different compound classes); (c) tautomerism should be absent (for simplest possible NMR spectra); (d) 1:1 stoichiometry (i.e., avoids diastereomers); and, most importantly, (e) proton NMR spectra have split resonances where $\Delta\delta$ is proportional to guest *ee*. To fulfil these multifarious conditions, we returned to the **OxP** system since it is unique amongst calix[4]pyrrole-type compounds in its regioselective alkylation at pyrrolic nitrogen atoms [75]. N-alkylation at N_{21} and N_{23} leads to one isomer of the di-N-substituted product and does not cause changes to the molecular form, i.e., $\mathbf{OxPBz_2}$, N_{21},N_{23}-dibenzyl-5,10,15,20-*tetrakis* (3,5-di-*t*-butyl-4-oxocyclohexa-2,5-dienylidene)porphyrinogen, maintains a saddle-shaped conformation suitable for host–guest interactions. This molecule also fulfils many of our design requirements: there is a single binding site for a hydrogen-bonded guest with N-alkylation restricting/preventing tautomerism. $\mathbf{OxPBz_2}$ is also difficult to protonate, and splitting of the relevant peaks for enantiomeric excess reporting is present, even at ambient temperatures. Importantly, the interactions of this host are based purely on hydrogen bonding, making it useful for *ee* estimation over a much wider range of analytes, including alcohols, amines, amino acid derivatives, and ketones.

Compounds of the type $\mathbf{OxPBz_2}$ are excellent examples of what we have come to refer to as prochiral solvating agents (*pro*-CSAs, see Figure 6a) [43,76]. If a single enantiomer guest (Figure 6b) is added to $\mathbf{OxPBz_2}$ in solution, there occurs a symmetrical splitting of the relevant reporter resonances of $\mathbf{OxPBz_2}$ (Figure 6c). Chiral guests interact with $\mathbf{OxPBz_2}$ by

H-bonding at pyrrolic NH groups, leading to a downfield shift of the NH peak (Figure 6c). Considering the conformation of the host and macrocycle rigidity, the distance between the guest binding site and the CH reporter groups is critical. CH groups responsible for sensing activity have different sensitivities (i.e., magnitude of $\Delta\delta$) depending on the guest (Figure 6c). **OxPBz$_2$** contains four groups with potential for sensing activity at different spatial positions and distances from the binding site so that the splitting of peaks due the CH reporter groups is highly likely to result where a chiral guest binds to **OxPBz$_2$**.

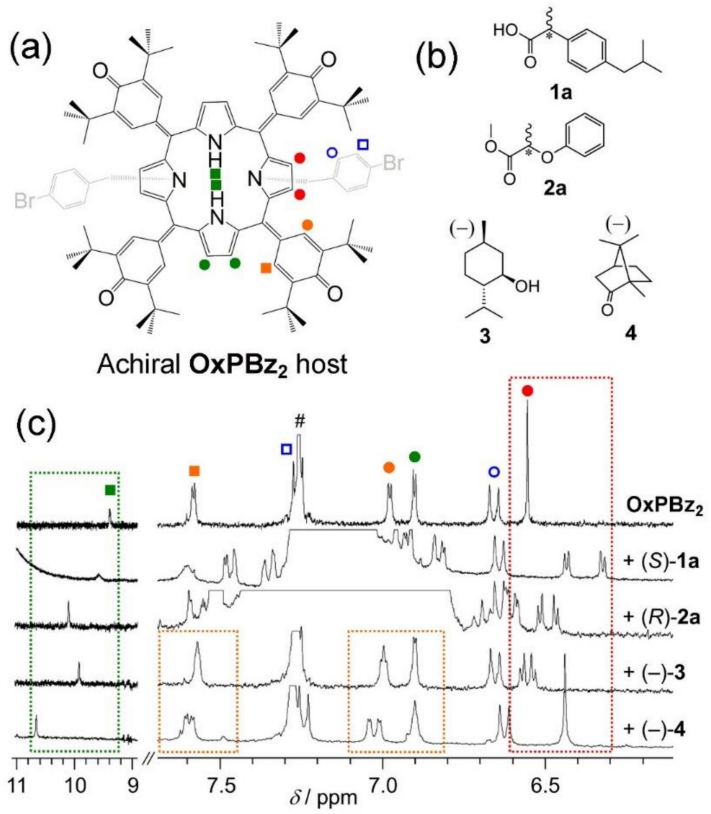

Figure 6. (**a**) Structure of the achiral host **OxPBz$_2$**. Colored shapes denote the proton resonances in (c). (**b**) Selected chiral guests. Ibuprofen (**1a**), 2-phenoxypropionic acid methyl ester (**2a**), (−)-menthol ((−)-**3**), (−)-camphor ((−)-**4**). (c) ^{1}H NMR spectra of **OxPBz$_2$** ($CDCl_3$, 0.7 mM) with ca. 400 eq. of the chiral guests indicated. Adapted with permission from ref. [43]. Copyright 2013 Labuta et al. Published by Springer Nature under a Creative Commons Attribution 3.0 International License http://creativecommons.org/licenses/by/3.0/ (access date: 6 September 2021).

If a chiral guest binds to **OxPBz$_2$,** the resulting non-equivalence of protons A and B (Figure 7a,b) is broken as indicated since certain orientations of guest are preferred (Figure 7c,d). When molecular mirror symmetry is broken (due to the presence of a chiral guest), protons A and B, which are initially enantiotopic, become diastereotopic, yielding non-identical and anisochronous chemical shifts (Figure 7b). Diastereomers are not formed, due to the relative positions of protons A and B in the molecule, which is also the reason why the intensities of the peaks observed at any arbitrary *ee* are identical. The appearance of two second-order doublets is a consequence of the proximity of protons A and B, which then undergo a vicinal scalar ^3J-coupling.

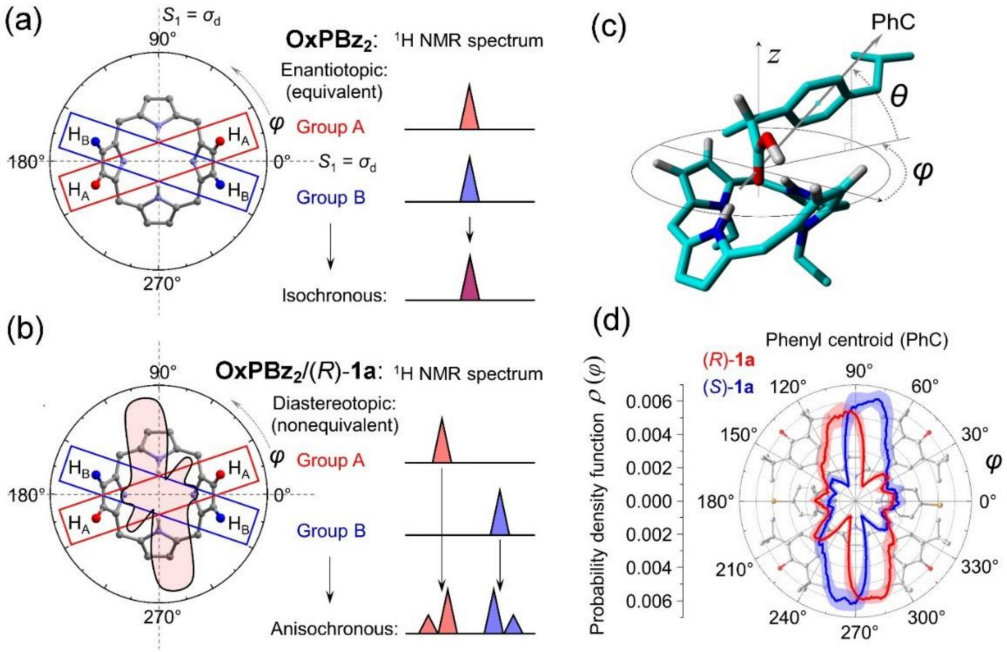

Figure 7. (**a**) Symmetry scheme of uncomplexed **OxPBz$_2$** host molecule and the corresponding shape of NMR spectra of pyrrolic reporting protons A and B. (**b**) Symmetry scheme of **OxPBz$_2$** host complexed with (*R*)-**1a** with resulting nonequivalent A and B protons due to the symmetry breaking upon the complexation. The dissymmetrizing "chiral field" (light red shading) induced by (*R*)-**1a** was calculated by molecular dynamics (MD) in (c,d). Corresponding NMR spectral pattern of A and B protons is also shown. (**c**) The reference system (ϕ and θ) of **OxPBz$_2$** and **1a** used for MD calculation. (**d**) Plots of probability density functions (ϕ components) as obtained from MD for **OxPBz$_2$**·(*R*)-**1a** (red line) and **OxPBz$_2$**·(*S*)-**1a** (blue line) complexes. Adapted with permission from Ref. [43]. Copyright 2013 Labuta et al. Published by Springer Nature under a Creative Commons Attribution 3.0 International License http://creativecommons.org/licenses/by/3.0/ (access date: 6 September 2021).

In practical usage, *pro*-CSA **OxPBz$_2$** has some interesting features. Repetitive estimations of the *ee* of an analyte (e.g., where pharmaceutical development requires it) can be undertaken after construction of a suitable calibration curve. The *pro*-CSA reagents can also be applied for continuous estimation of *ee* in racemization or enantioenrichment reactions (e.g., the Soai reaction [77]). Additionally, conventional CSA methods require a particular CSA reagent for each type of analyte (e.g., carboxylic acids suggest chiral amines). **OxPBz$_2$** is an extremely versatile *pro*-CSA since a wide variety of different analytes lead to useful chemical shift non-equivalence, due to H-bonding interactions of the analyte with the probe molecule [43]. As a result of chiral information transfer from analyte to **OxPBz$_2$**, and subsequent readout of the *ee* information from the host's NMR resonances, **OxPBz$_2$** might be modified for the retrieval of chiral information from, for instance, ^{19}F NMR spectra, where the analyte and solvent resonances would not interfere. Finally, it should be noted that *ee* sensing involving **OxPBz$_2$** does not depend on diastereomer formation [43]. This counterintuitive feature is a symptom of what might be termed "*dynamic diastereotopic mirroring*" based on the symmetry of the host and its sensing reporter groups together with a fast guest exchange [43].

3. Extension to Small Molecules—The Case of Benzylamine

The mechanism of action of the **OxP**, **OxPBz$_2$** and **TPP** systems relies on the diastereotopicity of proton resonances in rapidly exchanging guest–host systems. In principle, similar situations might exist in many host–guest pairs, and we sought these, eventually discovering such activity in the case of selected benzylamine/2-phenylpropionic acid com-

binations [45]. Certain small prochiral (non-macrocyclic) molecules exhibit the splitting of ^{1}H-NMR resonances in isotropic media, which is dependent on the *ee* of a chiral analyte. Notably, this occurs when compounds contain a phenoxy group at the α-position to the carboxyl group in either a chiral acid (as the analyte) or a prochiral acid (as the probe). Some prochiral amines, such as benzylamine (**BA**), 1-aminopropane or piperidine, exhibit clear splitting of certain ^{1}H-NMR resonances dependent on the *ee* of 2-phenoxypropionic acid (**PA**) even at room temperature. Similarly, ^{1}H-NMR resonances prochiral phenoxyacetic acid (**PAA**) are split in the presence of chiral 1-phenylethylamine (**PEA**), reflecting its *ee* [45]. If the phenoxy group is not present at the appropriate position, the NMR response is either weak or undetectable, even at low temperatures where intermolecular interactions ought to be enhanced. **BA**/**PA** complexation characteristics were investigated comprehensively by measuring NMR titrations, Fourier transform infrared (FTIR) and vibrational circular dichroism (VCD) spectra, X-ray crystallography and DFT calculations to establish the host–guest interaction mechanism.

The X-ray structure of the complex (Figure 8) reveals multiple points of interaction (ionic, H-bonds, CH-π) that affect the form of the **BA**/**PA** complex. These points promote the intra-complex transfer of magnetic anisotropy, leading to NMR peak splitting in spectra obtained from the solution state. Thus, while the **BA**/**PA** complex is a particular example of the prochiral phenomenon, it is possible that the development of design rules for prochiral solvating agents (*pro*-CSAs) will lead to a general method for the estimation of *ee* by NMR. The general principle behind the **BA**/**PA** NMR spectra splitting effect, its X-ray structure, line-drawing illustration and typical NMR spectra are shown in Figure 8.

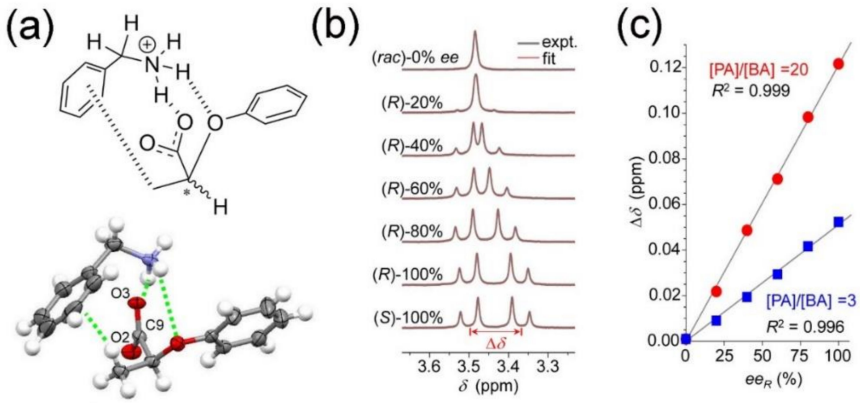

Figure 8. (**a**) Salt complex of benzylammonium (**BA**) with 2-phenoxypropionic acid ((*R*)-**PA**) and its X-ray crystal structure. (**b**) Benzylic CH_2 region of the ^{1}H-NMR spectra of **BA** (10 mM) in the presence of (*R*)-**PA** (200 mM) at various *ee* at room temperature in $CDCl_3$ solution. (**c**) Dependencies of benzylic CH_2 splitting $\Delta\delta$ of **BA** on the *ee* of **PA** (obtained at two different relative concentrations of **PA**/**BA** noted) illustrating the linear relationship of *ee* and $\Delta\delta$. Adapted with permission from Ref. [45]. Copyright 2018 American Chemical Society.

4. Coordination Complexes

Having observed the simplest cases for *ee* estimation using small molecule probes, we then considered other mechanisms for guest or 'ligand' exchange. The term 'ligand' introduces a broad field of coordination complexes with transition (and other) metal cations. The coordinated groups containing electronegative atoms (i.e., ligands) are capable of exchanging with other entities present in solution. This provides a source of instability for the relevant coordination complexes that might be exploited in host–guest exchange type processes applicable for the present subject of enantiomer excess estimation.

The complex **L**·2Zn·3**C** (where Zn = zinc (II), **L** = prochiral ligand, **C** = an exchangeable co-ligand, in this case, acetate-type ligands) undergoes splitting of the proton NMR resonances of **L**, which is symmetrical and proportional to *ee* of the chiral co-ligand guest (here again, we have used 2-phenoxypropionic acid (**PA**) as a model guest) [47]. In con-

trast to the previous **BA**/**PA** case, the chiral guest complex is highly stable, even at low concentrations so that the relevant NMR resonances remain split, even when the sample is diluted. This is because coordinate bonds are usually much stronger than hydrogen bonds [78] (standard chiral-solvating agents are often coordination complexes containing chiral ligands [40,79–81]). Thus, the *pro*-CSA concept might be broadened by considering the same activity of coordination complexes. However, the averaging of chemical shift non-equivalency (required for operation of *pro*-CSA agents) occurs only under a fast exchange regime of the chiral guests at a *pro*-CSA binding site [82,83]. Thus, at the outset of this work, it was not clear that the incorporation of coordination bonds into a *pro*-CSA sensing system would lead to useful activity because strong guest binding of ligands usually allows only slow exchange [84].

Ultimately, we were able to report the primary example of a *pro*-CSA reagent involving the coordination-bond-based guest exchange [47]. Ligand, **L**, a Salen [85], incorporates a benzylic CH_2, which is prochiral, appended to a Zn (II) coordination complex containing exchangeable co-ligands, **C**, (initially acetate (AcO) to be replaced with chiral ligands of **PA**). While Salen ligands generally have C_2 symmetry, in this case, because only certain space groups (C_s, C_{2v}, D_{2d}, S_4) can result in the splitting of NMR signals by a prochiral mechanism, one of the Salen salicylic substituents was replaced by benzyl, leading to a breaking of its symmetry to C_s (Figure 9a). The benzylic CH_2 of **L** is prochiral, and thus, its NMR resonance is capable of acting as an *ee* reporter group for chiral guests bound to the Zn (II) cation in **L**·2Zn·3**C** following the exchange of co-ligands **C**. (Figure 9a). The X-ray structure of **L**·2Zn·3**C** contains two chiral enantiomers (Figure 9b), which is the static solid-state structure. In solution, on the other hand, the concurrent rapid interconversion of chirality (by inversion of the amine functionality) and fast exchange of co-ligands (**C**s) leads to the coordination complex **L**·2Zn·3**C** being established as a *pro*-CSA. The ^{1}H-NMR peak, due to benzylic CH_2 in a three-way mixture containing ligand **L**, Zn $(AcO)_2$ and **PA,** undergoes splitting according to *ee* of the chiral guest (Figure 9c) with linear dependence of $\Delta\delta$ (of benzylic CH_2 of **L**) on *ee* of **PA** (Figure 9d). No splitting of NMR signals was found for solutions containing only **L** and **PA**, indicating the indispensable role of Zn (II) in this system. In this case, the *ee*-dependence of NMR peak splitting in the coordination complex remains, even in dilute solutions since chiral guests remain associated, i.e., the complex is stable with the chiral guest being more strongly bound than acetate. The host–guest complex stability is, thus, in contrast to the previously reported hydrogen-bonded or acid-base host–guest systems described here. This report provided the first evidence that the fast ligand exchange in the coordination complex can be used for *pro*-CSA activity. The findings provide new insight into metal–ligand complex chirality transfer events, and also establish an important new area of investigation for coordination complexes in the context of chirality involving dynamic coordination bonds.

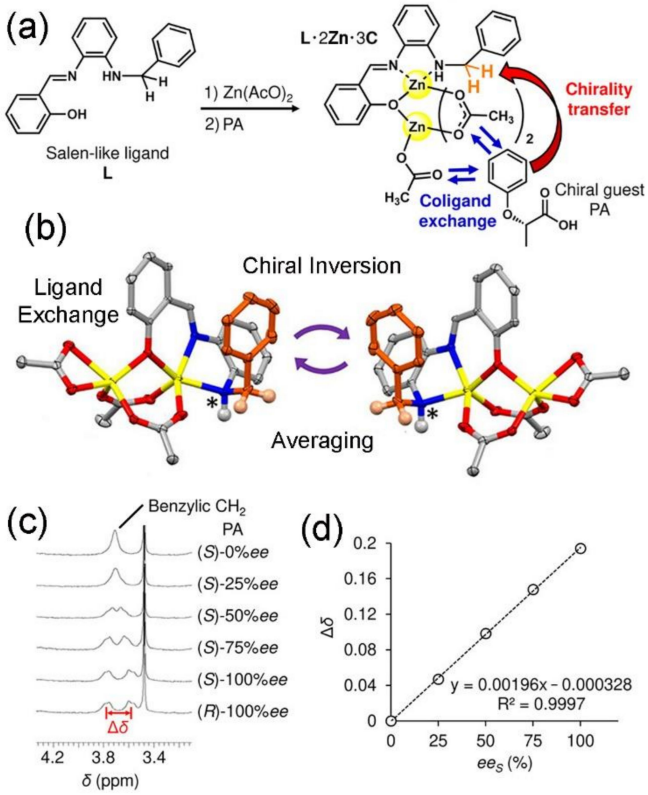

Figure 9. (**a**) Mechanism of chirality transfer in a mixture containing the species **L**, **Zn** (**AcO**)$_2$ and **PA**. (**b**) Benzylic CH_2 resonance in the ^{1}H-NMR spectra (in $CDCl_3$, 25 °C) of **L**·2**Zn**·3**C** in the presence of **PA** at different *ee*. (**c**) The magnitude of splitting ($\Delta\delta$; from (b)) depends linearly on *ee* of **PA**. (**d**) X-ray crystal structure of **L**·2**Zn**·3**AcO** showing possible sources of signal averaging in NMR spectra, including chiral inversion (at amine atom) and ligand exchange. Adapted with permission from Ref. [47]. Copyright 2020 American Chemical Society.

Finally, we will mention coordination complexes of a chiral porphyrin dimer based on the binaphthyl system. This completes the circle of study on this subject for us since our initial interest of the molecular chiral sensing concept was stimulated by considering the initial reports from Borovkov, Inoue, Berova and Nakanishi, amongst others [32,35,67–69]. Our receptor includes *meso*-alkyl-substituted porphyrins because of recent synthetic projects in our laboratories and the perception that these are more suitable than tetraphenylporphyrins (**TPP**s) for guest binding studies, where the proximity of chromophores in a dimer might be critical to the response of the dimeric receptors.

We designed a chiral porphyrin dimer probe **(TAPZn)$_2$Binaph** (Figure 10) [46] based on the following: (a) it should contain a chiral entity (for the differentiation of stereoisomers); in this case, we have used the 1,1′-binaphthyl group, (b) host–guest interactions based on porphyrin units (i.e., by metal cation coordination or imine group protonation), (c) improved guest binding, due to the use of *meso*-tetraalkylporphyrins, and (d) be based on diporphyrin tweezers, similar to those developed by Borokov, Berova and others [32,35,67–69]. Perceived difficulties in the synthesis of *meso*-*n*-tetraalkylporphyrins [86] have disfavored their use in these systems, although effective methods for their preparation in good yields are now available [87].

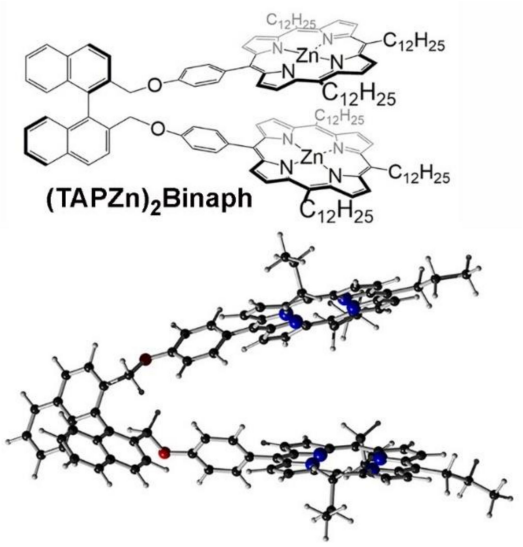

Figure 10. Structure of the 1,1′-binaphthyl porphyrin dimer receptor **$(TAPZn)_2Binaph$** [46] used for multichannel spectroscopic estimation of *ee*. The lower panel shows an energy minimized structure of the corresponding free base porphyrin with *meso*-*n*-propyl groups (instead of *meso*-*n*-dodecyl) for clarity.

Porphyrin dimers are well established as probes for chiral analyses. Therefore, in this case, we had the additional benefit of a comparison of our new results with a very similar and recently reported *meso*-tetraphenylporphyrin (**TPP**) analogue of our system [88], which was also used for chiral analysis. Lu et al. [88] observed easy discrimination of the enantiomers of cyclohexane-1,2-diamine (**CHDA**), using their porphyrin-substituted 1,1′-binaphthyl dimer host, and was mirrored in our report using NMR spectroscopy and other methods. Our report includes additional analytical possibilities for *ee* determination by using electronic spectrophotometry including UV-vis, CD and fluorescence emission methods. To make UV-vis observations more effective, *meso*-alkylporphyrins were preferred over **TPP,** due to the advantage of shifting the electronic absorption maximum of the **$(TAPZn)_2Binaph$** dimer host to higher energy relative to that of the diamine complex, making it easier for the construction of calibration diagrams for *ee* analyses. This work also illustrated that fluorescence emission can be applied for *ee* determination, using porphyrin dimers, although photo-induced demetallation of the metalloporphyrin dimer host complicated this procedure [46]. Based on these results, we predict that in the near future, other more suitable tetrapyrroles or dimers thereof will be eventually found to establish effective fluorescent *ee* sensors.

5. Conclusions

This review chronologically summarizes our synthetic and methodological advancements in detecting enantiomeric excess (*ee*) of various chiral analytes based on rapid analyte exchange in host–guest systems. We have shown that achiral porphyrin-based macrocyclic hosts, such as **OxP**, **TPP**, **$OxPBz_2$** or **$(TAPZn)_2Binaph$,** can be utilized as potent *ee* sensors for various guests in two modes of operation, i.e., forming host–guest complexes by acid–base or hydrogen-bonding interactions. From these results, we have deduced general requirements for the symmetry groups that any potential *pro*-CSA host must have and the limits for the exchange rate of chiral guests at the host's binding site. With this in mind, we have extended our study to non-macrocyclic molecules, including very simple prochiral molecules, such as benzylamine (**BA**), and also more complicated zinc (II) coordination complexes (**L·2Zn·3AcO**). These systems exhibit unique activity based on the structures of the probe molecules, such as concentration independence and a broad range of temperatures allowed for *ee* analyses. During the development of *pro*-CSA sensing methods, we have improved the synthetic design of host molecules and investigated various interactions

and modes of operation in a broad range of temperatures in order to clarify the fundamental aspects of the *ee*-sensing mechanisms. Some interesting advantages are presented by the *pro*-CSA approach, such as rapid estimation of *ee,* using a simple NMR method without necessity for derivatization, excellent scope of analytes (esters, alcohols, amides, acids, etc.) and the use of an achiral probe, whose presence, while monitoring an asymmetric reaction, does not bias the chiral outcome. Disadvantages of the method include a necessity to construct calibration curves and poor precision in the *ee* values, especially in mixtures close to the racemic condition. This ongoing research provides a new point of view on *ee* sensing using the NMR technique since it is not based on the formation of diastereomers. We believe that the utility and versatility of our *pro*-CSA approach will find its niche industrial, pharmaceutical or research applications.

Author Contributions: Conceptualization, J.L. and J.P.H.; writing—original draft preparation, J.L., S.I. and J.P.H.; writing—review and editing, D.T.P., K.T., H.S., L.H. and K.A.; visualization, J.L., S.I., D.T.P. and J.P.H. All authors have read and agreed to the published version of the manuscript.

Funding: This research was funded by JSPS KAKENHI Grant No. JP16H06518 (Coordination Asymmetry) and Grant No. 19K05229.

Institutional Review Board Statement: Not applicable.

Informed Consent Statement: Not applicable.

Acknowledgments: This work was partly supported by the World Premier International Research Center Initiative (WPI Initiative), MEXT, Japan.

Conflicts of Interest: The authors declare no conflict of interest.

References

1. Hutt, A.J. Drug Chirality and Its Pharmacological Consequences. In *Introduction to the Principles of Drug Design and Action*; Smith, H.J., Williams, H., Eds.; CRC Press: Boca Raton, FL, USA, 2006.
2. Jacobsen, E.N.; Pfaltz, A.; Yamamoto, H. *Comprehensive Organic Catalysis*; Jacobsen, E.N., Pfaltz, A., Yamamoto, H., Eds.; Springer: New York, NY, USA, 1999.
3. Heitbaum, M.; Glorius, F.; Escher, I. Asymmetric heterogeneous catalysis. *Angew. Chem. Int. Ed.* **2006**, *45*, 4732–4762. [CrossRef]
4. Yoon, T.P.; Jacobsen, E.N. Privileged chiral catalysts. *Science* **2003**, *299*, 1691–1693. [CrossRef]
5. Maeda, K.; Morino, K.; Okamoto, Y.; Sato, T.; Yashima, E. Mechanism of helix induction on a stereoregular poly((4-carboxyphenyl)acetylene) with chiral amines and memory of the macromolecular helicity assisted by interaction with achiral amines. *J. Am. Chem. Soc.* **2004**, *126*, 4329–4342. [CrossRef] [PubMed]
6. Ishi-i, T.; Crego-Calama, M.; Timmerman, P.; Reinhoudt, D.N.; Shinkai, S. Enantioselective formation of a dynamic hydrogen-bonded assembly based on the chiral memory concept. *J. Am. Chem. Soc.* **2002**, *124*, 14631–14641. [CrossRef]
7. Kondo, T.; Oyama, K.; Yoshida, K. Chiral molecular recognition on formation of a metalloanthocyanin: A supramolecular metal complex pigment from blue flowers of Salvia patens. *Angew. Chem. Int. Ed.* **2001**, *40*, 894–897. [CrossRef]
8. Hill, J.P.; Shrestha, L.K.; Ishihara, S.; Ji, Q.; Ariga, K. Self-assembly: From amphiphiles to chromophores and beyond. *Molecules* **2014**, *19*, 8589–8609. [CrossRef] [PubMed]
9. Ishihara, S.; Labuta, J.; van Rossom, W.; Ishikawa, D.; Minami, K.; Hill, J.P.; Ariga, K. Porphyrin-based sensor nanoarchitectonics in diverse physical detection modes. *Phys. Chem. Chem. Phys.* **2014**, *16*, 9713–9746. [CrossRef] [PubMed]
10. Li, M.; Ishihara, S.; Ji, Q.; Akada, M.; Hill, J.P.; Ariga, K. Paradigm shift from self-assembly to commanded assembly of functional materials: Recent examples in porphyrin/fullerene supramolecular systems. *Sci. Tech. Adv. Mater.* **2012**, *13*, 053001. [CrossRef]
11. Siegel, J.S. (Ed.) *Supramolecular Stereochemistry*; Springer Netherlands: Dordrecht, The Netherlands, 1995.
12. Karnik, A.V.; Hasan, M. *Stereochemistry: A Three-Dimensional Insight*; Elsevier: Amsterdam, The Netherlands, 2021.
13. Schurig, V. Chiral separations using gas chromatography. *TrAC Trends Anal. Chem.* **2002**, *21*, 647–661. [CrossRef]
14. Okamoto, Y.; Ikai, T. Chiral HPLC for efficient resolution of enantiomers. *Chem. Soc. Rev.* **2008**, *37*, 2593–2608. [CrossRef] [PubMed]
15. Teixeira, J.; Tiritan, M.E.; Pinto, M.M.M.; Fernandes, C. Chiral stationary phases for liquid chromatography: Recent developments. *Molecules* **2019**, *24*, 865. [CrossRef]
16. Armstrong, D.W. Optical isomer separation by liquid chromatography. *Anal. Chem.* **1987**, *59*, 84A–91A. [CrossRef]
17. Pietrusiewicz, K.M.; Borkowski, M.; Strzelecka, D.; Kielar, K.; Kicińska, W.; Karevych, S.; Jasiński, R.; Demchuk, O.M. A general phenomenon of spontaneous amplification of optical purity under achiral chromatographic conditions. *Symmetry* **2019**, *11*, 680. [CrossRef]

18. Pirkle, W.H.; Sikkenga, D.L.; Pavlin, M.S. Nuclear magnetic resonance determination of enantiomeric composition and absolute configuration of γ-lactones using chiral 2,2,2,-trifluoro-1-(9-anthryl)ethanol. *J. Org. Chem.* **1977**, *42*, 384–387. [CrossRef]
19. Demchuk, O.M.; Świerczynska, W.; Pietrusiewicz, K.M.; Woźnica, M.; Wójcik, D.; Frelek, J. A convenient application of the NMR and CD methodologies for the determination of enantiomeric ratio and absolute configuration of chiral atropoisomeric phosphine oxides. *Tetrahedron Asymmetry* **2008**, *19*, 2339–2345. [CrossRef]
20. Pakulski, Z.; Demchuk, O.M.; Kwiatosz, R.; Osiński, P.W.; Świerczynska, W.; Pietrusiewicz, K.M. The classical Kagan's amides are still practical NMR chiral shift reagents: Determination of enantiomeric purity of P-chirogenic phospholene oxides. *Tetrahedron Asymmetry* **2003**, *14*, 1459–1462. [CrossRef]
21. Mizuno, Y.; Aida, T.; Yamaguchi, K. Chirality-memory molecule: Crystallographic and spectroscopic studies on dynamic molecular recognition events by fully substituted chiral porphyrins. *J. Am. Chem. Soc.* **2000**, *122*, 5278–5285. [CrossRef]
22. Nieto, S.; Lynch, V.M.; Anslyn, E.V.; Kim, H.; Chin, J. High-throughput screening of identity, enantiomeric excess, and concentration using MLCT transitions in CD spectroscopy. *J. Am. Chem. Soc.* **2008**, *130*, 9232–9233. [CrossRef] [PubMed]
23. Sato, H. A new horizon for vibrational circular dichroism spectroscopy: A challenge for supramolecular chirality. *Phys. Chem. Chem. Phys.* **2020**, *22*, 7671–7679. [CrossRef] [PubMed]
24. Kubo, Y.; Maeda, S.; Tokita, S.; Kubo, M. Colorimetric chiral recognition by a molecular sensor. *Nature* **1996**, *382*, 522–524. [CrossRef]
25. Zhu, L.; Anslyn, E.V. Facile quantification of enantiomeric excess and concentration with indicator-displacement assays: An example in the analyses of α-hydroxyacids. *J. Am. Chem. Soc.* **2004**, *126*, 3676–3677. [CrossRef]
26. Tsubaki, K.; Nuruzzaman, M.; Kusumoto, T.; Hayashi, N.; Wang, B.-G.; Fuji, K. Visual enantiomeric recognition using chiral phenolphthalein derivatives. *Org. Lett.* **2001**, *3*, 4071–4073. [CrossRef]
27. James, T.D.; Sandanayake, K.R.A.S.; Shinkai, S. Chiral discrimination of monosaccharides using a fluorescent molecular sensor. *Nature* **1995**, *374*, 345–347. [CrossRef]
28. Matsushita, M.; Yoshida, K.; Yamamoto, N.; Wirsching, P.; Lerner, R.A.; Janda, K.D. High-throughput screening by using a blue-fluorescent antibody sensor. *Angew. Chem. Int. Ed.* **2003**, *42*, 5984–5987. [CrossRef] [PubMed]
29. Mei, X.; Wolf, C. Enantioselective sensing of chiral carboxylic acids. *J. Am. Chem. Soc.* **2004**, *126*, 14736–14737. [CrossRef]
30. Yu, S.; Pu, L. Pseudoenantiomeric fluorescent sensors in a chiral assay. *J. Am. Chem. Soc.* **2010**, *132*, 17698–17700. [CrossRef] [PubMed]
31. Mirri, G.; Bull, S.D.; Horton, P.N.; James, T.D.; Male, L.; Tucker, J.H.R. Electrochemical method for the determination of enantiomeric excess of binol using redox-active boronic acids as chiral sensors. *J. Am. Chem. Soc.* **2010**, *132*, 8903–8905. [CrossRef]
32. Rekharsky, M.V.; Yamamura, H.; Inoue, C.; Kawai, M.; Osaka, I.; Arakawa, R.; Shiba, K.; Sato, A.; Young, H.K.; Selvapalam, N.; et al. Chiral recognition in cucurbituril cavities. *J. Am. Chem. Soc.* **2006**, *128*, 14871–14880. [CrossRef] [PubMed]
33. Borovkov, V.V.; Lintuluoto, J.M.; Inoue, Y. Supramolecular chirogenesis in zinc porphyrins: Mechanism, role of guest structure, and application for the absolute configuration determination. *J. Am. Chem. Soc.* **2001**, *123*, 2979–2989. [CrossRef]
34. Kubo, Y.; Ohno, T.; Yamanaka, J.-I.; Tokita, S.; Iida, T.; Ishimaru, Y. Chirality-transfer control using a heterotopic zinc(II) porphyrin dimer. *J. Am. Chem. Soc.* **2001**, *123*, 12700–12701. [CrossRef]
35. Li, X.; Tanasova, M.; Vasileiou, C.; Borhan, B. Fluorinated porphyrin tweezer: A powerful reporter of absolute configuration for *erythro* and *threo* diols, amino alcohols, and diamines. *J. Am. Chem. Soc.* **2008**, *130*, 1885–1893. [CrossRef]
36. Huang, X.F.; Fujioka, N.; Pescitelli, G.; Koehn, F.E.; Williamson, R.T.; Nakanishi, K.; Berova, N. Absolute configurational assignments of secondary amines by CD-sensitive dimeric zinc porphyrin host. *J. Am. Chem. Soc.* **2002**, *124*, 10320–10335. [CrossRef] [PubMed]
37. Nuñez, M.d.C.; Gallo, M.A.; Espinosa, A.; Campos, J.M. Rapid Development of Chiral Drugs in the Pharmaceutical Industry. In *New Developments in Medicinal Chemistry*; Taft, C.A., Ed.; Bentham Science Publisher: Sharjah, United Arab Emirates, 2010; Volume 1, pp. 95–113.
38. Halpern, J.; Trost, B. Asymmetric catalysis (highlighting PNAS special issue). *Proc. Nat. Acad. Sci. USA* **2004**, *101*, 5347. [CrossRef]
39. Dale, J.A.; Dull, D.L.; Mosher, H.S. alpha.-Methoxy-.alpha.-trifluoromethylphenylacetic acid, a versatile reagent for the determination of enantiomeric composition of alcohols and amines. *J. Org. Chem.* **1969**, *34*, 2543–2549. [CrossRef]
40. Parker, D. NMR determination of enantiomeric purity. *Chem. Rev.* **1991**, *91*, 1441–1457. [CrossRef]
41. Wenzel, T.J.; Wilcox, J.D. Chiral reagents for the determination of enantiomeric excess and absolute configuration using NMR spectroscopy. *Chirality* **2003**, *15*, 256–270. [CrossRef] [PubMed]
42. Shundo, A.; Labuta, J.; Hill, J.P.; Ishihara, S.; Ariga, K. Nuclear magnetic resonance signaling of molecular chiral information using an achiral reagent. *J. Am. Chem. Soc.* **2009**, *131*, 9494–9495. [CrossRef]
43. Labuta, J.; Ishihara, S.; Šikorský, T.; Futera, Z.; Shundo, A.; Hanyková, L.; Burda, J.V.; Ariga, K.; Hill, J.P. NMR spectroscopic detection of chirality and enantiopurity in referenced systems without formation of diastereomers. *Nat. Commun.* **2013**, *4*, 2188. [CrossRef]
44. Labuta, J.; Futera, Z.; Ishihara, S.; Kouřilová, H.; Tateyama, Y.; Ariga, K.; Hill, J.P. Chiral guest binding as a probe of macrocycle dynamics and tautomerism in a conjugated tetrapyrrole. *J. Am. Chem. Soc.* **2014**, *136*, 2112–2118. [CrossRef]
45. Ishihara, S.; Labuta, J.; Futera, Z.; Mori, S.; Sato, H.; Ariga, K.; Hill, J.P. NMR spectroscopic determination of enantiomeric excess using small prochiral molecules. *J. Phys. Chem. B* **2018**, *122*, 5114–5120. [CrossRef]

46. Payne, D.T.; Chahal, M.K.; Březina, V.; Webre, W.A.; Ariga, K.; D'Souza, F.; Labuta, J.; Hill, J.P. Diporphyrin tweezer for multichannel spectroscopic analysis of enantiomeric excess. *Front. Chem. Sci. Eng.* **2020**, *14*, 28–40. [CrossRef]
47. Takimoto, K.; Ishihara, S.; Labuta, J.; Březina, V.; Hill, J.P.; Ariga, K.; Sumita, M.; Mori, S.; Sato, H. Enantiomeric excess dependent splitting of NMR signal through co-ligand dynamic exchange in a coordination complex. *J. Phys. Chem. Lett.* **2020**, *11*, 8164–8169. [CrossRef]
48. Milgrom, L.R. The facile aerial oxidation of a porphyrin. *Tetrahedron* **1983**, *39*, 3895–3898. [CrossRef]
49. Hill, J.P.; Hewitt, I.J.; Anson, C.E.; Powell, A.K.; McCarthy, A.L.; Karr, P.A.; Zandler, M.E.; D'Souza, F. Highly non-planar, electron deficient, N-substituted tetraoxocyclohexadienylidene porphyrinogens: Structural, computational, and electrochemical investigations. *J. Org. Chem.* **2004**, *69*, 5861–5869. [CrossRef]
50. Golder, A.J.; Milgrom, L.R.; Nolan, K.B.; Povey, D.C. 5,10,15,20-*Meso-tetrakis*(3,5-di-*t*-butyl-4-quinomethide) porphyrinogen: A highly puckered tetrapyrrolic macrocycle from the facile aerial oxidation of a phenolic porphyrin. *J. Chem. Soc. Chem. Commun.* **1989**, *22*, 1751–1753. [CrossRef]
51. Dong, S.K.; Sessler, J.L. Calix[4]pyrroles: Versatile molecular containers with ion transport, recognition, and molecular switching functions. *Chem. Soc. Rev.* **2015**, *44*, 532–546.
52. Hill, J.P.; Schumacher, A.L.; D'Souza, F.; Labuta, J.; Redshaw, C.; Elsegood, M.R.J.; Aoyagi, M.; Nakanishi, T.; Ariga, K. A chromogenic indicator for anion reporting based on an N-substituted oxoporphyrinogen. *Inorg. Chem.* **2006**, *45*, 8288–8296. [CrossRef] [PubMed]
53. Chahal, M.K.; Payne, D.T.; Labuta, J.; Karr, P.A.; D'Souza, F.; Ariga, K.; Hill, J.P. Selective phase transfer reagents (OxP-crowns) for chromogenic detection of nitrates especially ammonium nitrate. *Chem. Eur. J.* **2020**, *26*, 13177–13183. [CrossRef]
54. Ishihara, S.; Labuta, J.; Šikorský, T.; Burda, J.V.; Okamoto, N.; Abe, H.; Ariga, K.; Hill, J.P. Colorimetric detection of trace water in tetrahydrofuran using *N*,*N*′-substituted oxoporphyrinogens. *Chem. Commun.* **2012**, *48*, 3933–3935. [CrossRef]
55. Ishihara, S.; Iyi, N.; Labuta, J.; Deguchi, K.; Ohki, S.; Tansho, M.; Shimizu, T.; Yamauchi, Y.; Naito, M.; Abe, H.; et al. Naked-eye discrimination of methanol and ethanol using composite film of oxoporphyrinogen and layered double hydroxide. *ACS Appl. Mater. Interfaces* **2013**, *5*, 5927–5930. [CrossRef]
56. Chahal, M.K.; Labuta, J.; Březina, V.; Karr, P.A.; Matsushita, Y.; Webre, W.A.; Payne, D.T.; Ariga, K.; D'Souza, F.; Hill, J.P. Knock-on synthesis of tritopic calix[4]pyrrole host for enhanced anion interactions. *Dalton Trans.* **2019**, *48*, 15563–15596. [CrossRef]
57. Shundo, A.; Ishihara, S.; Labuta, J.; Onuma, Y.; Sakai, H.; Abe, M.; Ariga, K.; Hill, J.P. Colorimetric visualization of acid-base equilibria in non-polar solvent. *Chem. Commun.* **2013**, *49*, 6870–6872. [CrossRef]
58. D'Souza, F.; Subbaiyan, N.K.; Xie, Y.; Hill, J.P.; Ariga, K.; Ohkubo, K.; Fukuzumi, S. Anion-complexation-induced stabilization of charge separation. *J. Am. Chem. Soc.* **2009**, *131*, 16138–16146. [CrossRef] [PubMed]
59. Chahal, M.K.; Liyanage, A.; Alsaleh, A.Z.; Karr, P.A.; Hill, J.P.; D'Souza, F. Anion-enhanced excited state charge separation in a spiro-locked N-heterocycle-fused push-pull zinc porphyrin. *Chem. Sci.* **2021**, *12*, 4925–4930. [CrossRef] [PubMed]
60. Chahal, M.K.; Liyanage, A.; Gobeze, H.B.; Payne, D.T.; Ariga, K.; Hill, J.P.; D'Souza, F. Supramolecular ultrafast energy and electron transfer in a directly Linked BODIPY-oxoporphyrinogen dyad upon fluoride ion binding. *Chem. Commun.* **2020**, *56*, 3855–3858. [CrossRef] [PubMed]
61. Chahal, M.K.; Gobese, H.B.; Webre, W.A.; Karr, P.A.; Payne, D.T.; Ariga, K.; D'Souza, F.; Hill, J.P. Electron and energy transfer in a porphyrin-oxoporphyrinogen-fullerene triad, ZnP-OxP-C_{60}. *Phys. Chem. Chem. Phys.* **2020**, *22*, 14356–14363. [CrossRef] [PubMed]
62. Chahal, M.K.; Velychkivska, N.; Webre, W.A.; Labuta, J.; Ishihara, S.; Ariga, K.; D'Souza, F.; Hill, J.P. Increasing the complexity of oxoporphyrinogen colorimetric sensing chromophores: N-alkylation and β-substitution. *J. Porphyrins Phthalocyanines* **2019**, *23*, 1184–1194. [CrossRef]
63. Chahal, M.K.; Payne, D.T.; Matsushita, Y.; Labuta, J.; Ariga, K.; Hill, J.P. Molecular Engineering of β-Substituted Oxoporphyrinogens for Hydrogen-Bond Donor Catalysis. *Eur. J. Org. Chem.* **2020**, *2020*, 82–90. [CrossRef]
64. Milgrom, L.R. *The Colors of Life*; Oxford University Press: Oxford, UK, 1997.
65. Scheer, H. *Chlorophylls*; CRC Press: Boca Raton, FL, USA, 1991.
66. Lewis, D.F.W. *Guide to Cytochromes P450*; Taylor and Francis: London, UK, 2002.
67. Proni, G.; Pescitelli, G.; Huang, X.F.; Nakanishi, K.; Berova, N. Magnesium tetraarylporphyrin tweezer: A CD-sensitive host for absolute configurational assignments of α-chiral carboxylic acids. *J. Am. Chem. Soc.* **2003**, *125*, 12914–12927. [CrossRef]
68. Balaz, M.; De Napoli, M.; Holmes, A.E.; Mammana, A.; Nakanishi, K.; Berova, N.; Purrello, R. A cationic zinc porphyrin as a chiroptical probe for Z-DNA. *Angew. Chem. Int. Ed.* **2005**, *44*, 4006–4009. [CrossRef]
69. Borovkov, V.V.; Fujii, I.; Muranaka, A.; Hembury, G.A.; Tanaka, T.; Ceulemans, A.; Kobayashi, N.; Inoue, Y. Rationalization of supramolecular chirality in a bisporphyrin system. *Angew. Chem. Int. Ed.* **2004**, *43*, 5481–5485. [CrossRef]
70. D'Souza, F.; Schumacher, A.L.; Hill, J.P.; Karr, P.A.; Zandler, M.E.; Xie, Y.; Ariga, K.; Sandanayaka, A.S.D.; Araki, Y.; Ito, O. Oxoporphyrinogens: From redox and spectroscopic probe for anion sensing to a platform for construction of supramolecular donor-acceptor conjugates. *Electrochem. Soc. Trans.* **2008**, *13*, 127–136. [CrossRef]
71. Hembury, G.A.; Borovkov, V.V.; Inoue, Y. Chirality-sensing supramolecular systems. *Chem. Rev.* **2008**, *108*, 1–73. [CrossRef] [PubMed]
72. Furusho, Y.; Kimura, T.; Mizuno, Y.; Aida, T. Chirality-memory molecule: A D_2-symmetric fully substituted porphyrin as a conceptually new chiral sensor. *J. Am. Chem. Soc.* **1997**, *119*, 5267–5268. [CrossRef]

73. Labuta, J.; Ishihara, S.; Shundo, A.; Arai, S.; Takeoka, S.; Ariga, K.; Hill, J.P. Chirality sensing by nonchiral porphines. *Chem. Eur. J.* **2011**, *17*, 3558–3561. [CrossRef] [PubMed]
74. Stone, A.; Fleischer, E.B. The molecular and crystal structure of porphyrin diacids. *J. Am. Chem. Soc.* **1968**, *90*, 2735–2748. [CrossRef]
75. Labuta, J.; Hill, J.P.; Elsegood, M.R.J.; Ariga, K. Synthesis of stable pseudotetrahedral supermolecules based on an oxoporphyrinogen. *Tetrahedron Lett.* **2010**, *51*, 2935–2938. [CrossRef]
76. Labuta, J.; Ishihara, S.; Ariga, K.; Hill, J.P. Dynamic processes in prochiral solvating agents (pro-CSAs) studied by NMR spectroscopy. *Symmetry* **2014**, *6*, 345–367. [CrossRef]
77. Soai, K.; Shibata, T.; Morioka, H.; Choji, K. Asymmetric autocatalysis and amplification of enantiomeric excess of a chiral molecule. *Nature* **1995**, *378*, 767–768. [CrossRef]
78. Lawrance, G.A. *Introduction to Coordination Chemistry*; John Wiley & Sons Ltd: Chichester, UK, 2009.
79. Zhao, Y.; Swager, T.M. Simultaneous chirality sensing of multiple amines by ^{19}F NMR. *J. Am. Chem. Soc.* **2015**, *137*, 3221–3224. [CrossRef] [PubMed]
80. Wang, W.; Xia, X.; Bian, G.; Song, L. A chiral sensor for recognition of varied amines based on ^{19}F NMR signals of newly designed rhodium complexes. *Chem. Comm.* **2019**, *55*, 6098–6101. [CrossRef]
81. Li, L.P.; Peng, H.L.; Ye, B.H. Chiral sensor for enantiomeric purity of amines, amino alcohols and amino esters based on bis-cyclometalated Ir(III) complex using ^{1}H NMR spectroscopy. *Inorg. Chim. Acta* **2018**, *482*, 691–697. [CrossRef]
82. Labuta, J.; Hill, J.; Ishihara, S.; Hanyková, L.; Ariga, K. Chiral sensing by nonchiral tetrapyrroles. *Acc. Chem. Res.* **2015**, *48*, 521–529. [CrossRef]
83. Labuta, J.; Ishihara, S.; Hill, J.P. *Meso*–tetraphenylporphine as prochiral solvating agent (pro–CSA): A physicochemical study. *J. Porphyrins Phthalocyanines* **2020**, *24*, 320–329. [CrossRef]
84. Burgess, J. *Inorganic Reaction Mechanism*; Royal Society of Chemistry: London, UK, 1971; Volume 2.
85. Cozzi, P.G. Metal-salen Schiff base complexes in catalysis: Practical aspects. *Chem. Soc. Rev.* **2004**, *33*, 410–421. [CrossRef] [PubMed]
86. Shinoda, T.; Onaka, M.; Izumi, Y. The reason why K10 is an effective promoter for meso-tetraalkylporphyrin synthesis. *Chem. Lett.* **1995**, *24*, 493–494. [CrossRef]
87. Plamont, R.; Kikkawa, Y.; Takahashi, M.; Kanesato, M.; Giorgi, M.; Shun, A.C.K.; Roussel, C.; Balaban, T.S. Nanoscopic imaging of meso-tetraalkylporphyrins prepared in high yields enabled by Montmorillonite K10 and 3 Å molecular sieves. *Chem. Eur. J.* **2013**, *19*, 11293–11300. [CrossRef]
88. Lu, W.; Yang, H.; Li, X.; Wang, C.; Zhan, X.; Qi, D.; Bian, Y.; Jiang, J. Chiral discrimination of diamines by a binaphthylene-bridged porphyrin dimer. *Inorg. Chem.* **2017**, *56*, 8223–8231. [CrossRef]